

## Original Full Length Article

# Digital tomosynthesis and high resolution computed tomography as clinical tools for vertebral endplate topography measurements: Comparison with microcomputed tomography

Daniel Oravec<sup>a</sup>, Abrar Quazi<sup>a</sup>, Angela Xiao<sup>a</sup>, Ellen Yang<sup>a</sup>, Roger Zuel<sup>a</sup>, Michael J. Flynn<sup>b</sup>, Yener N. Yeni<sup>a,\*</sup><sup>a</sup> Bone and Joint Center, Henry Ford Hospital, Detroit, MI, United States<sup>b</sup> Department of Radiology, Henry Ford Hospital, Detroit, MI, United States

## ARTICLE INFO

## Article history:

Received 17 February 2015

Revised 7 July 2015

Accepted 24 July 2015

Available online 26 July 2015

## Keywords:

Vertebral bodies

Endplate topography

Digital tomosynthesis

Microcomputed tomography

Computed tomography

## ABSTRACT

Endplate morphology is understood to play an important role in the mechanical behavior of vertebral bone as well as degenerative processes in spinal tissues; however, the utility of clinical imaging modalities in assessment of the vertebral endplate has been limited. The objective of this study was to evaluate the ability of two clinical imaging modalities (digital tomosynthesis, DTS; high resolution computed tomography, HRCT) to assess endplate topography by correlating the measurements to a microcomputed tomography ( $\mu$ CT) standard. DTS, HRCT, and  $\mu$ CT images of 117 cadaveric thoracolumbar vertebrae (T10–L1; 23 male, 19 female; ages 36–100 years) were segmented, and inferior and superior endplate surface topographical distribution parameters were calculated. Both DTS and HRCT showed statistically significant correlations with  $\mu$ CT approaching a moderate level of correlation at the superior endplate for all measured parameters ( $R^2_{Adj} = 0.19–0.57$ ), including averages, variability, and higher order statistical moments. Correlation of average depths at the inferior endplate was comparable to the superior case for both DTS and HRCT ( $R^2_{Adj} = 0.14–0.51$ ), while correlations became weak or non-significant for higher moments of the topography distribution. DTS was able to capture variations in the endplate topography to a slightly better extent than HRCT, and taken together with the higher speed and lower radiation cost of DTS than HRCT, DTS appears preferable for endplate measurements.

© 2015 Elsevier Inc. All rights reserved.

## 1. Introduction

Morphological features of human vertebral body endplates have been shown to be associated with important determinants of bone fragility and degenerative diseases of the spine. For instance, endplate thickness, curvature, and statistical moments of endplate topography distributions have been shown to be associated with vertebral load magnitude and distribution, microstructural properties of the underlying trabecular bone, vertebral failure strain and energy and intervertebral disc degeneration [1–6]. Microcomputed tomography ( $\mu$ CT) is typically used in such studies to produce a high resolution 3-dimensional depiction of vertebral endplate microarchitecture. However,  $\mu$ CT is only suitable in a laboratory setting with *in vitro* specimens due to size limitations and high radiation dose. Measurement of endplate topography using clinically available imaging modalities could improve assessment of vertebral bone quality in a clinical setting. To date, assessment of vertebral endplate using clinical imaging modalities has been limited to measurements such as density, thickness, and gross shape patterns [7–10].

Tomosynthesis was developed as a method to avoid superposition of objects present in conventional radiographic imaging and has evolved since its conception in the 1930s [11] through film [12] and fluoroscopy [13,14] techniques. Advances in flat panel digital detectors have realized a technology called digital tomosynthesis (DTS) [15]. Digital tomosynthesis is a tomographic imaging modality in which a series of projection images are acquired over a limited arc, with the X-ray source pivoting and translating opposite the direction of a flat panel detector encased in the scanning bed. Musculoskeletal DTS delivers 1/5th the dose or less than that of CT [16–18]. Tomosynthesis reconstructions of the spine are formed in the sagittal or coronal planes, in contrast with CT which produces an axial image with high slice thickness along the superior–inferior direction. Topographic features of the endplate surface are thus captured in-plane with a resolution of approximately 0.24 mm in DTS, rather than the axial resolution of 0.9 mm for HRCT; however, the out of plane slice sensitivity in DTS is about 3 mm [17, 19]. Taken together, these features suggest that tomosynthesis might be a preferred clinical imaging modality for geometric analysis of the vertebral endplate.

The current study aims to correlate comparable measures of endplate topography between  $\mu$ CT, digital tomosynthesis (DTS) and high resolution computed tomography (HRCT) in order to assess the viability of endplate topography measurement in a clinical imaging modality.

\* Corresponding author at: HFHS/IBio, Attn.: Bone & Joint Center, 6135 Woodward, Detroit, MI 48202, United States.

## 2. Methods

Human cadaveric thoraco-lumbar spines were acquired under local IRB approval from tissue banks and four vertebral bodies (T10, T11, T12, L1) were harvested from 42 donors. Donors with a history of HIV, hepatitis, diabetes, renal failure, metastatic cancer, osteomalacia, hyperparathyroidism, Paget's disease of bone, spine surgery, cause of death involving trauma, and corticosteroid, anticonvulsant or bisphosphonate use were not included. Vertebral bodies were dissected, soft tissue and posterior elements were removed, and specimens were stored wrapped in saline-soaked gauze at  $-20^{\circ}\text{C}$  until scanning was performed. The donor set consisted of 23 men and 19 women all between the ages of 36 and 100 years. Collectively, the vertebrae of these donors formed a set of 117 bones.

Specimens were mounted and consistently aligned in a custom radiolucent scanning tank filled with 0.9% saline and scanned using DTS (Shimadzu Sonialvision Safire II) and high resolution CT (Siemens Sensation 64). Scanning in saline-filled Lucite tanks ( $14 \times 14 \times 40$  cm) was performed so as to establish bone–water contrast similar to the bone–tissue contrast encountered in vivo. Consistent endplate alignment was ensured using a radiolucent clamping system such that the anterior–posterior (AP) and lateral–medial (LM) anatomical directions were aligned to the reconstructed CT image axes. Tomosynthesis scans were performed in two orientations: AP (series of coronal slices) and LM (series of sagittal slices). The same specimens were scanned using a custom-built  $\mu\text{CT}$  system and reconstructed at an isotropic voxel size of  $40\ \mu\text{m}$ . The  $\mu\text{CT}$  system used in the study was based on the hardware, data acquisition, and reconstruction methods of the  $\mu\text{CT}$  system that has been previously described [20]. The presently operating system uses a Kevex 16-Watt X-ray source with a 9-micron focal spot, a  $1888 \times 1408$ -pixel Varian PaxScan 2520 flat panel digital X-ray detector with 127-micron pitch, a Newport precision rotational stage, and control software running under Windows XP.

For HRCT images, a single, unique threshold value in Hounsfield Units was manually determined for each vertebra as the minimum value that delineates bone from soft tissue. The threshold value was used within a custom segmentation algorithm to produce a closed surface gray value mask of the vertebral body [21], from which volume masks separating cortical and cancellous bone were segmented using

a previously-described semi-automatic method [22]. The segmentation algorithm consists of dilating the binarized vertebral image twice (closing porosity within and on the surface of the vertebra), applying a median filter (connecting surfaces and smoothing processing artifacts), and eroding back twice. The resulting volume, a solid mask image of the whole vertebral body, was further cropped into separate volumes representing superior and inferior endplates. The topography of each endplate was assessed by creating a 2D height map in which each pixel represented the depth from a fixed plane (the first slice) to the first encounter of bone along the superior–inferior axis using the TopoJ plugin for ImageJ (Fig. 1) [23]. The depth distribution (background and holes were eliminated from the analysis) was recorded into a text file in which each row represented a single pixel in 2D height map. The average (Av), standard deviation, skewness (Skew), and kurtosis (Kurt) of the depth measurements were calculated to represent up to the fourth moment of the topography distribution [24]. A high average depth may represent the presence of large surface concavity or many deep pits, while standard deviation of the endplate topography distribution is a measure of endplate surface overall depth variation. Low average and standard deviation of depth are characteristic of a smooth surface. Skewness measures the symmetry of the depth distribution, and may be used as a measure of surface spikiness. Kurtosis measures the spread of the depth distribution (distribution sharpness may be influenced by features such as steep epiphyseal ring or a small number of steep peaks or valleys on the endplate surface). Kurtosis and skewness are understood to affect surface pressure distributions in engineering materials, such that high values of each result in high load bearing ratio and maximum contact pressure [25]. For instance, the combination of high kurtosis and low skewness has been shown to reduce friction [26].

A similar process was performed for DTS images. A global threshold value was manually determined to delineate bone from soft tissue and air. Due to a blurring effect in the highest and lowest slices of the DTS reconstructions, a central substack of 25 slices (25 mm) was created and the image was binarized in ImageJ using the recorded threshold value (Fig. 2a). Binarized images were cropped into separate volumes representing superior and inferior endplates. Depth distributions were again calculated for DTS endplate images and distribution statistics were calculated from DTS depth measurements. Additionally, depth

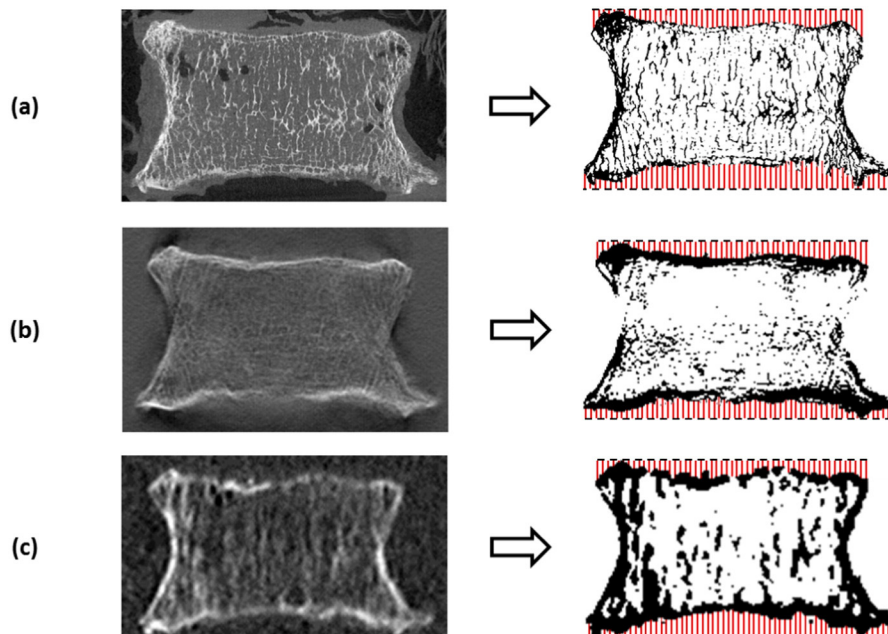


**Fig. 1.** Images were thresholded and depth distributions calculated from a fixed plane (dashed lines) at the superior and inferior endplates. Comparison of images taken from sagittal plane in similar regions from (a)  $\mu\text{CT}$ , (b) DTS (AP), and (c) HRCT. Images are resized to show detail at comparable scale.

Download English Version:

<https://daneshyari.com/en/article/5889282>

Download Persian Version:

<https://daneshyari.com/article/5889282>

[Daneshyari.com](https://daneshyari.com)